JOURNAL OF SOLID STATE CHEMISTRY 103, 441–446 (1993)

Incommensurate Superlattice in Mo-Substituted $Bi_4V_2O_{11}$

R. N. VANNIER,* G. MAIRESSE, F. ABRAHAM, AND G. NOWOGROCKI

Laboratoire de Cristallochimie et Physicochimie du solide (L.C.P.S.), URA CNRS 452, ENSCL, B.P. 108, 59652 Villeneuve d'Ascq Cedex, France

Received April 2, 1992; in revised form September 23, 1992; accepted September 25, 1992

A $Bi_2V_{(1-x)}Mo_xO_{(11+x)/2}$ solid solution derived from $Bi_4V_2O_{11}$ has been prepared and characterized with x up to 0.225. The ability to introduce Mo into the [V] site of $Bi_4V_2O_{11}$ leads to the stabilization of a β incommensurate phase at room temperature. © 1993 Academic Press, Inc.

Introduction

Depending on the temperature, $Bi_4V_2O_{11}$ exhibits three different polymorphs, α, β, and γ. Their crystal structures can be described in an orthorhombic "mean cell" $a_m \approx 5.53$, $b_m \approx 5.61$, and $c_m \approx 15.28$Å.

The α phase, stable at room temperature, is a superstructure with three times the a_m period, while the β form (appearing above 450°C) is a superstructure with doubling of the same a_m period. The high temperature γ phase is stable from 580°C up to the melting point (≈885°C) and its crystal structure is described in the *I4/mmm* space group with $a_{tetragonal} \approx \sqrt{2}/2a_m$ (*1*).

From a structural point of view $Bi_4V_2O_{11}$ can be formulated as $(Bi_2O_2)^{2+}$ $(VO_{3.5}\square_{0.5})^{2-}$ and therefore can be considered as derived from γBi_2MoO_6, the $n = 1$ member of the Aurivillius compounds $(Bi_2O_2)^{2+}$ $(A_{n-1}B_nO_{3n+1})^{2-}$ (*2*).

The disorder of all the atomic positions (except that of the O atoms of the (Bi_2O_2) sheets) and the oxygen vacancies in the perovskite type slabs lead to high anionic conductivity in this high temperature γ phase (*3*).

Several successful attempts at stabilizing the γ form at room temperature have already been performed by partial substitution of V^V by lower oxidation state cations such as Co, Ni, Cu, and Zn. This new family of compounds, designated as BIMEVOX, exhibits high oxide ion conductivities at low temperature (*3, 4*).

The purpose of this paper is to describe the results obtained by substitution of V^V by a higher oxidation state cation such as Mo^{VI}, the choice of Mo^{VI} being dictated by the obvious structural similitudes between BIMEVOX and Bi_2MoO_6.

Experimental

Samples with $Bi_2V_{(1-x)}Mo_xO_{(11+x)/2}$ composition were prepared by solid state reaction from stoichiometric amounts of the appropriate pure oxides: Bi_2O_3 (Aldrich, 99.9% degree of purity), V_2O_5 (Johnson

* To whom correspondence should be addressed.

0022-4596/93 $5.00

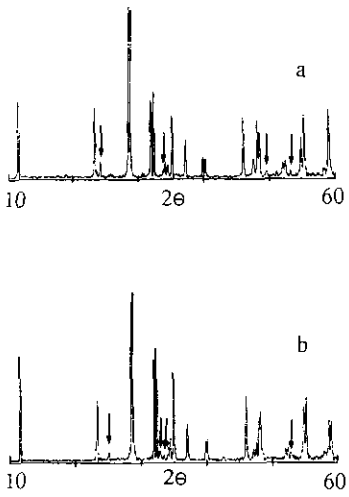

FIG. 1. X-ray powder diffraction patterns obtained for (a) $x = 0.025$, (b) $x = 0.075$ (arrows indicate superlattice reflections).

Matthey, 99.5%), and MoO_3 (Merck, 99.5%). After thorough mixing in an agate mortar, these oxides were preheated in a gold crucible at 600°C, reground, and calcinated at 820°C for 24 hr.

Single crystals were grown in a gold crucible from a melt corresponding to $x = 0.10$ nominal composition, cooled between

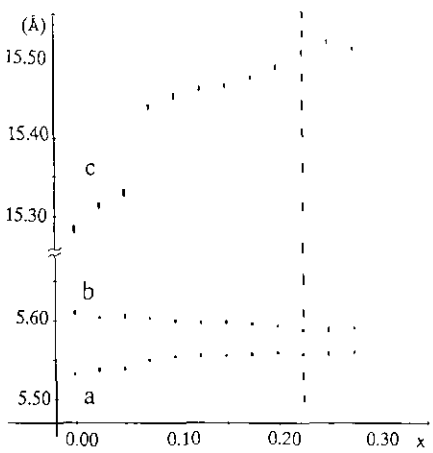

FIG. 2. Evolution of the "mean cell" parameters for the solid solution $Bi_2V_{1-x}Mo_xO_{(11+x)/2}$.

TABLE I

X-RAY POWDER PATTERN FOR $Bi_2V_{1-x}Mo_xO_{(11+x)/2}$ WITH $x = 0.025$ CORRESPONDING TO $a = 5.535(2) \times 3$; $b = 5.604(2)$; $c = 15.311(4)$Å

hkl	$2\Theta_{cal}$	$2\Theta_{obs}$	I/I_0
002	11.55	11.53	18
004*	23.22	23.30	17
311	23.31		
013	23.56	23.60	2
113*	**24.17**	**24.13**	**4**
313	28.61	28.61	100
020	31.91	31.92	18
600	32.32	32.32	20
220*	**33.73**	**33.80**	**2**
022	34.04	34.03	4
602	34.43	34.43	3
006	35.14	35.13	15
315	37.16	37.16	9
024	39.84	39.83	5
604	40.18	40.19	5
620	46.06	46.06	14
008*	47.47	47.59	5
317*	47.51		
622*	47.65		
026	48.19	48.19	13
606	48.48	48.50	11
226*	**49.50**	**49.56**	**2**
326*	51.11	51.09	2
331*	51.97	52.05	4
624*	52.20		
133*	**52.41**	52.44	4
911*	52.52		
426*	**53.29**	**53.24**	**2**
233*	**53.34**		
333	54.86	54.86	10
913	55.39	55.39	15
028	58.34	58.36	2
608	58.59	58.56	2
319*	59.11	59.12	16
626*	59.23		

Note. Heavy numerals correspond to superlattice reflections. Reflections marked with an asterisk were not used in the least-squares refinement of the mean cell parameters.

900°C and 800°C at 1°C/hr, and then to room temperature in the switched-off furnace.

Samples were studied by X-ray powder diffraction (Guinier–De Wolff camera and Siemens D5000 diffractometer using Cu$K\alpha$

TABLE II

X-RAY POWDER PATTERN FOR $Bi_2V_{1-x}Mo_xO_{(11+x)/2}$ WITH $x = 0.075$ CORRESPONDING TO $a = 5.550(1) \times 2$; $b = 5.602(1)$; $c = 15.443(2)$Å

hkl	$2\Theta_{cal}$	$2\Theta_{obs}$	I/I_0	*hklm*[a]	$2\Theta_{cal}$
002	11.45	11.46	25	0020	
004	23.02	23.03	4	0040	
211	23.26	23.26	14	1110	
113*	**24.80**	**24.98**	**2**	**113$\bar{1}$**	**24.99**
213	28.49	28.50	100	1130	
020	31.92	31.93	24	0200	
400	32.23	32.23	27	2000	
120*	**32.95**	**32.80**	**3**	**0201**	**32.81**
313*	**33.82**	**33.39**	**2**	**1131**	**33.41**
022	34.02	34.02	5	0220	
402	34.31	34.32	6	2020	
006	34.83	34.83	21	0060	
215	36.94	36.94	9	1150	
024	39.72	39.73	5	0240	
404	39.98	39.98	5	2040	
420	46.00	46.00	15	2200	
008*	47.03	47.13	3	0080	
217*	47.17			1170	
422	47.56	47.57	5	2220	
026	47.96	47.96	10	0260	
406	48.18	48.18	12	2060	
231*	51.96	52.02	3	1310	
424*	52.04			2240	
611*	52.37	52.42	3	3110	
133*	**52.75**	**52.80**	**2**	**133$\bar{1}$**	**52.85**
233	54.80	54.80	13	1330	
613	55.20	55.19	15	3130	
028	57.97	57.95	3	0280	
408	58.16	58.14	2	2080	
219	58.62	58.63	10	1190	
426	58.96	58.97	10	2260	

Note. Heavy numerals correspond to superlattice reflections. Reflections marked with an asterisk were not used in the least-squares refinement of the mean cell parameters.

[a] Four-integer indexation of the reflections in the mean cell.

radiation with a step size for the X-ray diffraction scans of 0.02° and a counting time at each step of 1.5 sec), DSC analysis (1090B Thermal Analyzer, Dupont Instruments), conductivity (Solartron 1170 Frequency Response Analyzer), and density measurements (Micromeritics Accupyc 1330 Pycnometer, 1 ml sample capacity). The way in which the complex impedance spectra were obtained has been previously described (*3*).

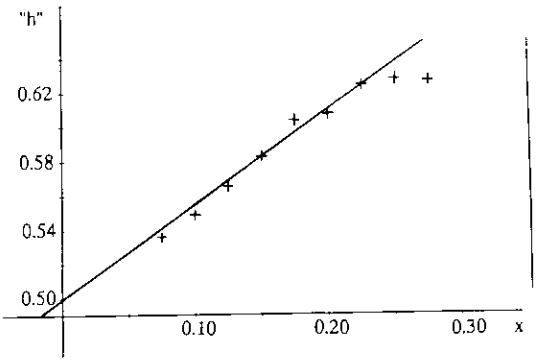

FIG. 3. Evolution of the "*h*" Miller index of the β supercell "1"1 3 reflection recalculated in the mean cell versus *x*.

Results and Discussion

A $Bi_2V_{(1-x)}Mo_xO_{(11+x)/2}$ solid solution based on $Bi_4V_2O_{11}$ is obtained over a limited range of x up to 0.225. For $x < 0.05$, the solid solution belongs to the α type $Bi_4V_2O_{11}$, while for $0.05 < x < 0.225$, it becomes of β type as revealed by X-ray powder diffraction (Fig. 1).

The results of least squares refinement of the mean cell parameters versus x are

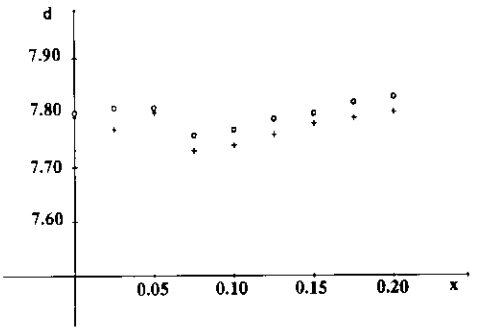

FIG. 4. Solid solution $Bi_2V_{1-x}Mo_xO_{(11+x)/2}$ densities versus *x*: (+) experimental, (○) calculated.

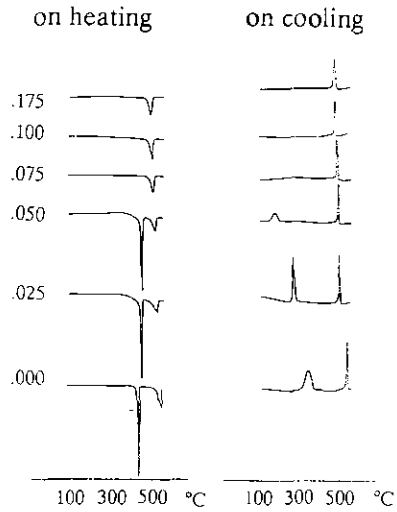

FIG. 5. DSC analyses on $Bi_2V_{1-x}Mo_xO_{(11+x)/2}$. Downward deflections of the curve correspond to endothermic reactions and upward deflections to exothermic reactions.

reported in Fig. 2. The cell remains orthorhombic within all the composition range but the $\alpha \rightarrow \beta$ type change is characterized by an important increase of the c parameter for x values greater than 0.05.

X-ray powder diffraction data for α and β corresponding to $x = 0.025$ and $x = 0.075$ are reported in Tables I and II, respectively: typically superlattice reflexions 113, 220, 226, 133, 426, and 233 are detected in the α phase, and 113, 120, 313, and 133 in the β-phase. In this β phase, the 113 superlattice reflexion ($2\Theta \approx 25°$) has the strongest intensity and moreover is situated in a 2Θ range with no close neighbor subcell fundamental reflection. It is therefore particularly suitable to detect some eventual evolution versus the x parameter.

The most striking feature is the poor fit between $2\Theta_{observed}$ and $2\Theta_{calculated}$ for this 113 reflection in the $2 \times a_m$ supercell. The reindexation of this peak in the mean cell gives rise to the new non-half-integer "h" Miller index values reported in Fig. 3. It is worthwhile to notice the linear variation of "h" value versus x. On one hand extrapolation of the straight line towards $x = 0$ leads to "h" ≈ 0.5 (within the experimental error) which corresponds to the $2 \times a_m$ supercell of unsubstituted $\beta Bi_4V_2O_{11}$. On the other hand, extrapolation toward upper x values gives the corresponding maximum $h = 0.625$ for $x = 0.225$, close to $x = 0.25$, which would correspond to an integer $h = 5$ value in an $8 \times a_m$ supercell (or a $4 \times a_\beta$ cell) when the ratio Mo/(V + Mo) $= \frac{1}{4}$.

Finally, the results of these X-ray diffraction studies from powder patterns of polycrystalline specimens with $0.05 < x < 0.225$ clearly indicate the stabilization, at room temperature, of an incommensurate β type phase. The coupling between the "h" Miller index and the Mo/V ratio is in agreement with a compositional modulation due to an ordering of the Mo atoms in the [V] sites along the a axis direction of the orthorhombic cell.

The reciprocal lattice vector can be written

$$G = ha_m^* + kb_m^* + lc_m^* + mq = H + mq,$$

where q is the modulation wave vector and H any basic reciprocal lattice vector.

In the considered case q can be expressed as $(1/p)\ a_m^*$, where p is the modulation period. In this description $q = 0.465\ a_m^*$ and $q = 0.375\ a_m^*$ (and consequently $p \approx 2.15$ and $p \approx 2.6$) for $x = 0.075$ and $x = 0.225$, respectively. The β-phase of Bi_4V_2O11 represents a commensurate superstructure with $p = 2$. A correct indexation (by utilizing the four-integer indexation scheme proposed by De Wolff (5)) of the satellite reflections in Table II should be $113\bar{1}$, 0201, 1131, and $133\bar{1}$, first order satellites reflections of respectively 113, 020, 113, and 133 fundamental ones. The introduction of that modulation gives rise to a good fit between $2\Theta_{observed}$ and $2\Theta_{calculated}$ (Table II) for these satellite reflections.

To complete these results, single crystals with Mo/V ratio corresponding to β type

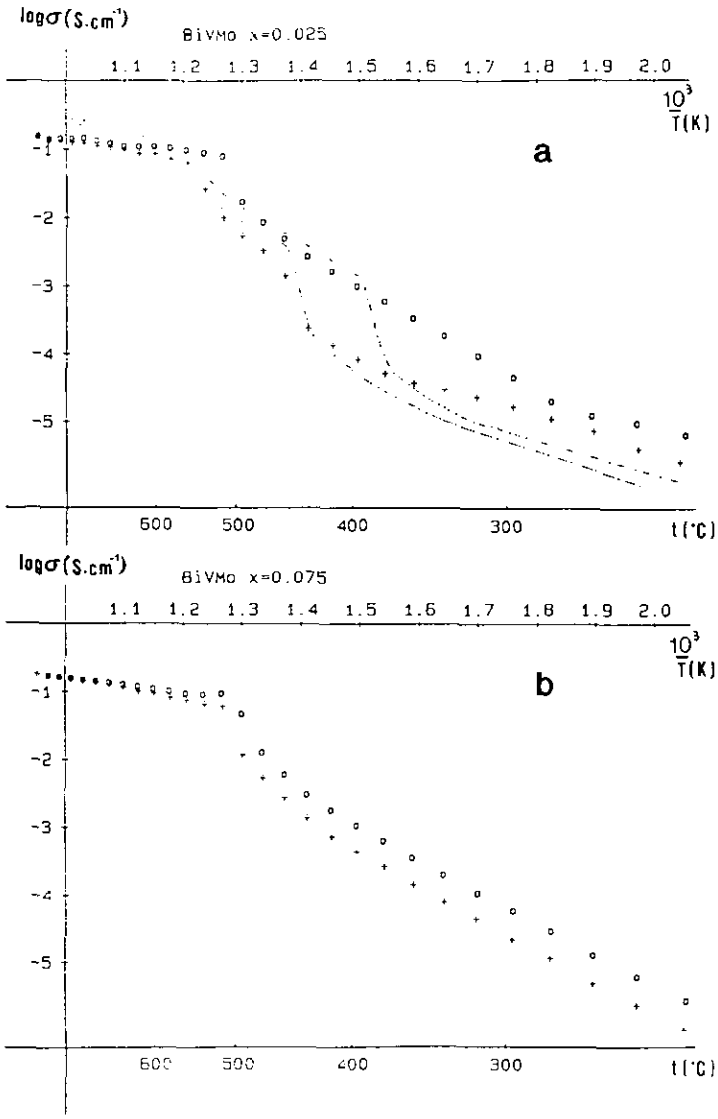

FIG. 6. Conductivity measurements of $Bi_2V_{1-x}Mo_xO_{(11+x)/2}$: (a) $x = 0.025$, (b) $x = 0.075$, (+) on heating, (O) on cooling. The $Bi_4V_2O_{11}$ curves are drawn in dotted lines.

phase stabilization were prepared by slow cooling from a melt with nominal formulation $x = 0.10$. The X-ray powder pattern obtained after grinding single crystals confirms the β type phase formation. One selected single crystal was studied by the Weissenberg method. By choosing the a parameter as the rotation axis ($a \approx 5.5$ Å in the mean cell), we observed on each side of the fundamental layers weak additional layers corresponding to a modulation wave $q \approx 0.44\, a_m^*$ (i.e., "h" ≈ 0.56). When compared to the "h" values reported in Fig. 3, this should correspond to a formulation

close to $x = 0.10$, in very good agreement with the starting composition. Moreover, no incommensurate peak was detected in the reciprocal planes $(0kl)$, $(1kl)$, and $(2kl)$, indicating a monodimensional modulation.

An additional interesting correlation was obtained between densities and compositions of these BIMEVOX compounds. The plot of density versus x (Fig. 4) shows that the solid solution density varies in accordance with the V/Mo substitution hypothesis.

The DSC curves are also in agreement with the previous structural observations (Fig. 5). For $x \leq 0.05$, we observed the typical $\alpha \rightleftarrows \beta$ and $\beta \rightleftarrows \gamma$ transitions of α type compounds, with a noticeable hysteresis of the $\beta \rightarrow \alpha$ (cooling process) transition temperature with increasing x values. When $x > 0.05$, only the $\beta \rightleftarrows \gamma$ transformation remained, due to the stabilization of β type compounds at 298 K.

The Arrhenius plots deduced from complex impedance spectroscopy data are drawn on Fig. 6, for $x = 0.025$ (α type compound) and $x = 0.075$ (β type compound). For $x = 0.025$ we can recognize the different α, β, and γ phases with a narrow β phase domain on heating but a much larger one on cooling, as already observed by DSC analysis. For $x = 0.075$, only the β and γ phases are identified with $\beta \rightleftarrows \gamma$ transition at about 500°C without hysteresis phenomenon (as in DSC). At $T < 500$°C (β phase domain), the activation energies are measured as 0.94 and 0.93 eV on heating and on cooling respectively. These values are in good agreement with the corresponding ones for the pure $\beta Bi_4V_2O_{11}$ phase (1.08 and 0.96 eV, respectively) and bring a further confirmation of the β structural type of these BIMOVOX compounds ($0.05 < x \leq 0.225$).

Moreover, the curves obtained for $x > 0.075$ are practically identical to those of the $x = 0.075$ compound reported on Fig. 6. As the V^V/Mo^{VI} substitution implies a decrease of the oxygen vacancies and as the conductivities remain practically the same throughout the composition range, we can conclude that the predominant parameter determining the conductivity performances is the structural arrangement characterizing the β type $Bi_4V_2O_{11}$. The number of O atoms/number of O vacancies ratio appears only as a second order parameter. Identical observations have frequently been emphasized during similar studies of other ionic superconductor families (6).

References

1. F. Abraham, J. C. Boivin, G. Mairesse, and G. Nowogrocki, *Solid State Ionics* **40–41**, 934–937 (1990).
2. B. Aurivillius, *Arkiv Kemi* **1**, 463 (1949).
3. F. Abraham, M. F. Debreuille-Gresse, G. Mairesse, and G. Nowogrocki, *Solid State Ionics* **28–30**, 529–532 (1988).
4. T. Iharada, A. Hammouche, J. Fouletier, and M. Kleitz, *Solid State Ionics* **48**, 257–265 (1991).
5. P. M. De Wolff, *Acta Crystallogr. Sect. A* **30**, 777–785 (1974).
6. P. Hagenmuller and W. Van Gool, "Solid Electrolytes," Academic Press, New York/San Francisco/London (1978).